Research Article

Received: 4 March 2025 Revised: 7 April 2025 Published online in Wiley Online Library:

(wileyonlinelibrary.com) DOI 10.1002/ps.8861

Discovery of novel benzoxazinone derivatives as promising protoporphyrinogen IX oxidase inhibitors

Hui Cai,[a] Xiao Zhang,[a] Dan Ling,[a] Meng Zhang,[a] Chen Pang,[a] Shi-Chao Ren,[a*] Zhichao Jin[a*] and Yonggui Robin Chi[a,b*]

Abstract

BACKGROUND: Protoporphyrinogen IX oxidase (PPO, EC 1.3.3.4) has emerged as a key target for developing new herbicides to protect crops from weeds. Herein, we disclose the development of two types of PPO inhibitors by modification of the benzoxazinone skeleton.

RESULTS: Two types of structurally novel benzoxazinone derivatives containing hydantoin or 1,2,3-triazole fragments were designed based on active substructure splicing and derivatization strategies. Systematic post-emergence herbicidal activity studies and crop selectivity assessments indicate that some of the compounds exhibit excellent herbicidal activity and crop safety. For instance, compound A1 shows highly effective herbicidal activity against all tested weeds at a dosage of 150 g ai/ha. Particularly, its herbicidal activity against broadleaf weeds is comparable to that of flumioxazin. Meanwhile, compound A1 exhibits superior safety for wheat and maize compared to flumioxazin within the 75–150 g ai/ha dosage range. Molecular docking studies revealed that compound A1 and flumioxazin occupy the same active cave within *Nicotiana tabacum* PPO (*Nt*PPO). It is noteworthy that the carbonyl group on the oxazolone moiety of both compound A1 and flumioxazin forms beneficial interactions with Arg-98 and Phe-392.

CONCLUSION: Our research indicates that benzoxazinone derivatives containing either hydantoin or 1,2,3-triazole fragments serve as a promising chemical scaffold for the development of novel PPO-inhibiting herbicides.

Supporting information may be found in the online version of this article.

Keywords: benzoxazinone derivatives; substructure splicing; derivatization; protoporphyrinogen IX oxidase; herbicides

ABBREVIATIONS

*Nt*PPO	*Nicotiana tabacum* PPO
FLU	Flumioxazin
MD	molecular dynamics
IC_{50}	half-maximal inhibitory concentration
NMR	nuclear magnetic resonance
SARs	structure–activity relationships
HRMS	high resolution mass spectrum
L.P.	*Lolium perenne*
E.C.	*Echinochloa crusgalli*
D.S.	*Digitaria sanguinalis*
A.R.	*Amaranthus retroflexus*
A.T.	*Abutilon theophrasti*
M.S.	*Medicago sativa*
MM_PBSA	Molecular mechanics_Poisson Boltzmann surface area
DMF	*N,N*-Dimethylformamide

1 INTRODUCTION

Protoporphyrinogen IX oxidase (PPO, EC 1.3.3.4) is one of the most important targets for developing new herbicides.[1–3] The chemical structures of PPO-inhibiting herbicides have become increasingly diverse since Rohm & Haas company developed the herbicide nitrofen in the mid-1960s. Some of them have been widely employed in agricultural production to control various weeds.[4,5] PPO-inhibiting herbicides are characterized by high efficiency and broad-spectrum herbicidal activity, exhibiting excellent weed

* *Correspondence to: S-C Ren, State Key Laboratory of Green Pesticides, Key Laboratory of Green Pesticide and Agricultural Bioengineering, Ministry of Education, Guizhou University, Huaxi District, Guiyang 550025, China. E-mail: scren@gzu.edu.cn (S-C Ren); Z Jin, State Key Laboratory of Green Pesticides, Key Laboratory of Green Pesticide and Agricultural Bioengineering, Ministry of Education, Guizhou University, Huaxi District, Guiyang 550025, China. E-mails: E-mail: zcjin@gzu.edu.cn (Z Jin); Y Robin Chi, State Key Laboratory of Green Pesticides, Key Laboratory of Green Pesticide and Agricultural Bioengineering, Ministry of Education, Guizhou University, Huaxi District, Guiyang 550025, China; E-mail: robinchi@ntu.edu.sg (YR Chi)*

a *State Key Laboratory of Green Pesticide, Key Laboratory of Green Pesticide and Agricultural Bioengineering, Ministry of Education, Guizhou University, Guiyang, China*

b *School of Chemistry, Chemical Engineering, and Biotechnology, Nanyang Technological University, Singapore, Singapore*

control for broadleaf weeds, certain grass weeds, and weeds that have developed resistance to glyphosate and acetolactate synthase (ALS) inhibitors.[6–8] To date, more than 30 commercial PPO inhibitors have been extensively utilized in various crop fields for weed management.[9]

The development of benzoheterocycle-based PPO-inhibiting herbicides, such as the derivatives based on benzoxazinone, benzothiazole, or benzoxazolinone cores,[10–14] has recently attracted much interest. These compounds generally possess novel chemical scaffolds and exhibit high herbicidal activity. However, although a number of benzoxazinone derivatives have been investigated, only limited members of them, such as flumioxazin (FLU), trifludimoxazin, and thidiazimin, have been developed and commercialized as PPO-inhibiting herbicides (Fig. 1(a)).[15] The thienopyrimidine-benzoxazin reported by Xi and co-workers can serve as an excellent PPO inhibitor with highly effective post-emergence herbicidal activity at 18.75–37.5 g ai/ha. Additionally, the crop safety assessment results indicate that the thienopyrimidine-benzoxazin could be developed as a herbicide for maize fields (Fig. 1(a)).[16]

Hydantoin, also known as imidazolidine-2,4-dione, is considered a valuable and privileged chemical scaffold in drug design and discovery.[17] Several compounds containing the hydantoin fragment were developed for medicinal applications. For example, phenytoin was used as an anticonvulsant and antiarrhythmic agent. Nilutamide was employed for the treatment of prostate cancer (Fig. 1(b)).[18–20] Besides, phenytoin, nilutamide, and FLU all contain a 2,4-dione moiety in their chemical structures. Another compelling feature of the hydantoin scaffold is that it can be synthesized through a straightforward cyclization reaction using the inexpensive amino acids and aniline compounds as the starting materials. Furthermore, this core structure is versatile for the introduction of various substituents.[17,21]

N-containing heterocycles are one class of the most commonly utilized pharmacophores in drug development.[22–25] Among them, 1,2,3-triazoles have attracted the attention of scientists due to their wide range of biological activities.[26–28] For example, both tazobactam and cefatrizine contain such structural fragments (Fig. 1(b)).[29,30] The azide-alkyne cycloaddition, which has become one of the significant methods in click chemistry due to its high efficiency and mild reaction conditions,[31,32] provides an important synthetic pathway for the development of 1,2,3-triazole compounds with various biological activities.

As a continuous effort in the development of novel pesticide structures in our laboratory,[33–35] we employed an active substructure splicing strategy to integrate hydantoin fragments into the benzoxazinone scaffold to design and synthesize a series of benzoxazinone derivatives containing hydantoin moieties as potential novel PPO inhibitors. Meanwhile, FLU was chosen as the reaction starting material, with its propargyl group utilized to react with various azide-containing substances to synthesize a series of benzoxazinone derivatives containing 1,2,3-triazole fragments through efficient cyclization reactions (Fig. 1(c)). Subsequently, we systematically assessed the herbicidal activity and crop selectivity of the synthetic compounds using a stem and leaf spray method. Additionally, molecular docking and the molecular mechanics Poisson-Boltzmann surface area (MM_PBSA) method were employed to investigate the binding modes and binding free energies of the highly effective herbicidal compounds with the PPO enzyme. This study offers a valuable example of innovation in target-based herbicide development through the strategies of structural linking and intermediate derivatization.

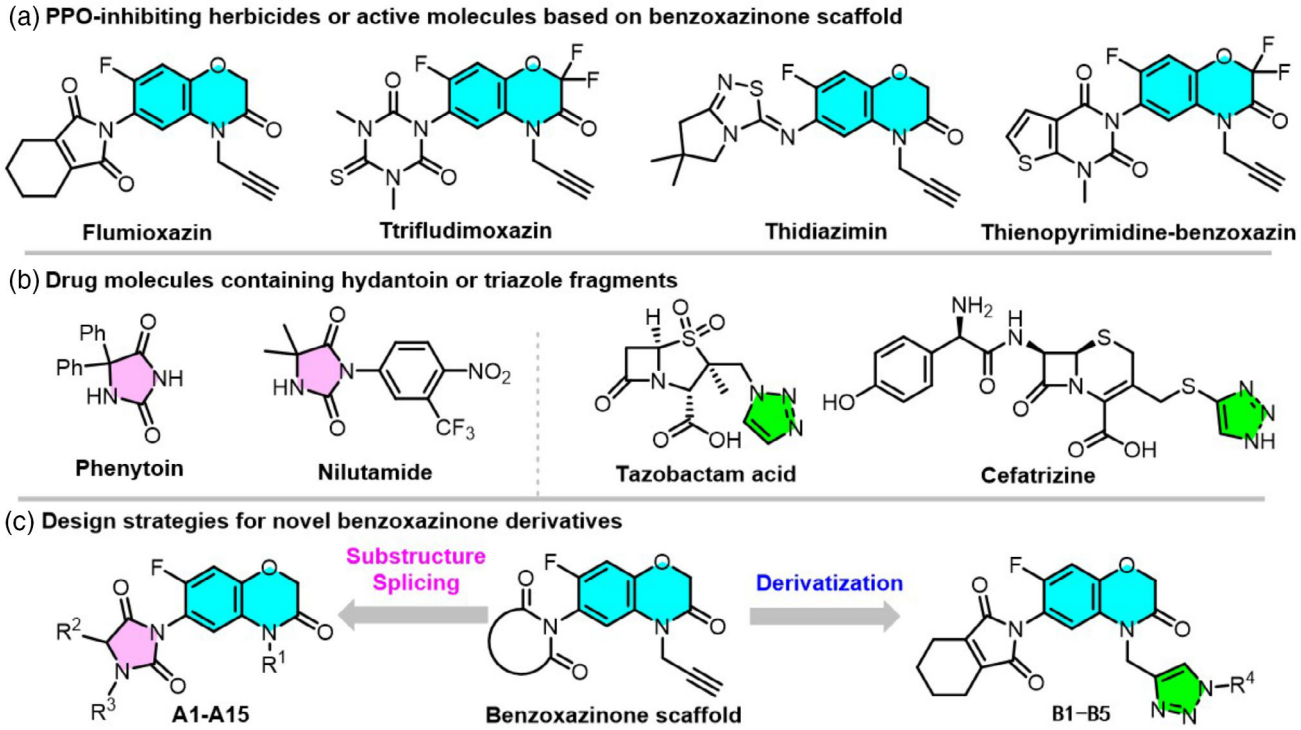

Figure 1. (a) PPO-inhibiting herbicides or active molecules based on benzoxazinone scaffold; (b) Drug molecules containing hydantoin or 1,2,3-triazole fragments; (c) Design strategies for novel benzoxazinone derivatives.

2 MATERIALS AND METHODS

2.1 Chemicals and instruments

All chemical reagents, solvents, and instruments employed in the experiments are enumerated and elucidated in the Supporting Information S1.

2.2 Synthetic chemistry

The synthetic routes for the target compounds **A1**-**A15** and **B1-B5** are shown in Fig. 2 and Fig. 3. The detailed synthetic methods and characterization data (^{1}H, ^{13}C, ^{19}F NMR spectra, HRMS dates, and melting points) for these compounds are outlined in the Supporting Information S1.

2.3 X-ray diffraction

Dissolve the target compound **A1** in a mixed solution of DMF and acetonitrile, and let the solution stand at room temperature. This process will precipitate colorless and block-shaped crystals. Suitable crystals will then be selected for structural confirmation using X-ray diffraction. The CIF file for compound **A1** was checked using the checkcif.iucr.org/ website, and the checkCIF reports were placed in the online version of this article. The supplementary crystallographic data for **A1** have been submitted and deposited in the Cambridge Crystallographic Data Centre (CCDC, http://www.ccdc.cam.ac.uk/) under deposition number 2355163. The crystal structure of **A1** is shown in Fig. 4.

2.4 Herbicidal activity

To systematically evaluate the post-emergence herbicidal activity of the target compound and intermediate **10a** against grass and broadleaf weeds, the following weeds were selected for the herbicidal activity tests: *Lolium perenne (L.P.)*, *Echinochloa crusgalli (E.C.)*, *and Digitaria sanguinalis (D.S.)*, *Amaranthus retroflexus (A.R.)*, *Abutilon theophrasti (A.T.)*, *and Medicago sativa (M. S.)*. Herbicidal activity tests and data evaluation were performed at application rates of 75 to 150 g ai/ha, referencing methods reported in previous literature.[36,37] Weed seeds were planted in plastic pots with an inner diameter of 8 cm and incubated in a greenhouse under alternating temperatures of 15 °C (night, 12 h) and 25 °C (day, 12 h). After approximately 2 weeks, both *Abutilon theophrasti* and *Digitaria sanguinalis* reached the third leaf stage. The target compound was dissolved in DMF and then diluted to the appropriate concentration with 0.1% Tween-80 before being evenly sprayed onto the stems and leaves of the weeds. The typical PPO inhibitor FLU was employed as a positive

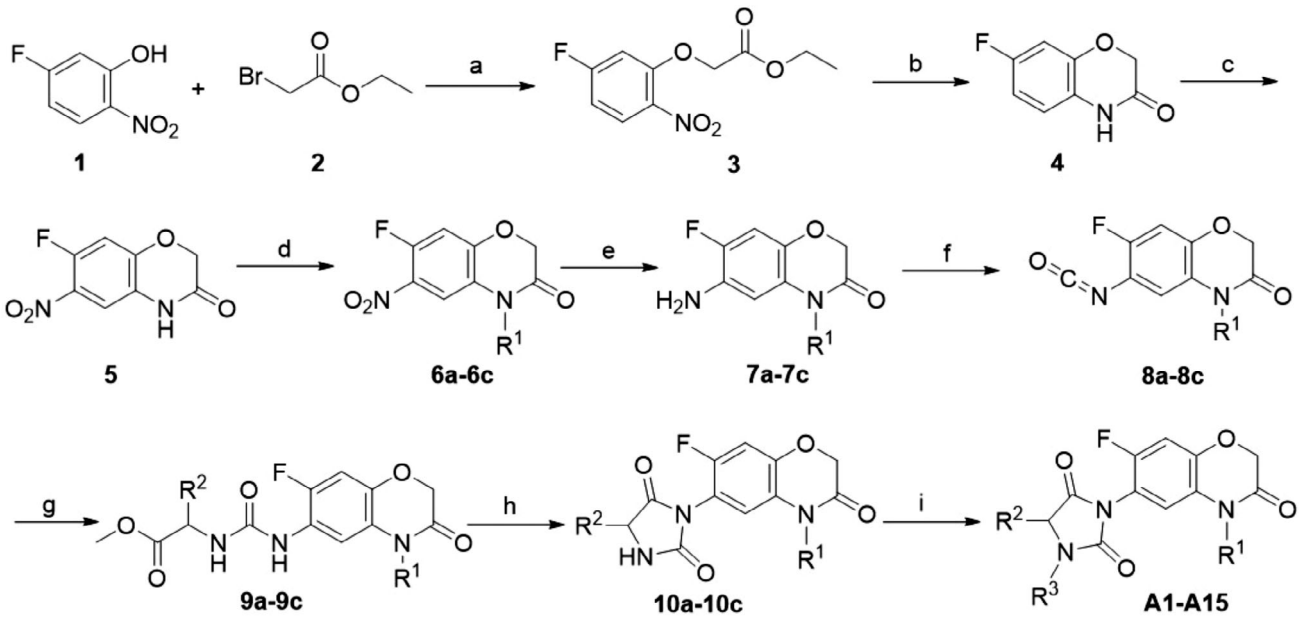

Figure 2. Synthetic procedures of compounds **A1-A15**. Reagents and conditions: (a) K_2CO_3, CH_3CN, reflux; (b) Fe, acetic acid, reflux; (c) HNO_3, H_2SO_4, 0 °C-r.t.; (d) R^1-X, Cs_2CO_3, DMF, r.t.; (e) Fe, NH_4Cl, C_2H_5OH (80%), reflux; (f) $CO(OCCl_3)_2$, Et_3N, 1,4-Dioxane, 0 °C to reflux; (g) Various amino acid methyl ester hydrochlorides (rac), Et_3N, 1,4-Dioxane, reflux; (h) 6 M HCl, CH_3OH, 80 °C; (i) R^3-X, Cs_2CO_3, DMF, 50 °C.

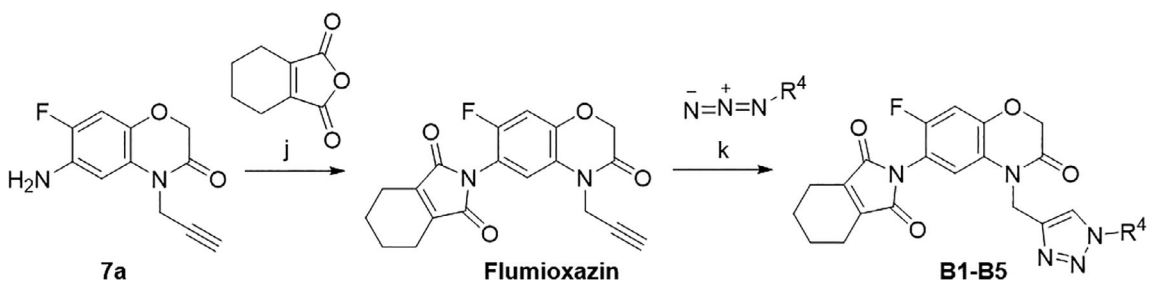

Figure 3. Synthetic procedures of compounds **B1-B5**. Reagents and conditions: (j) CH_3COOH, 80 °C; (k) CuI, 1,4-Dioxane, 80 °C.

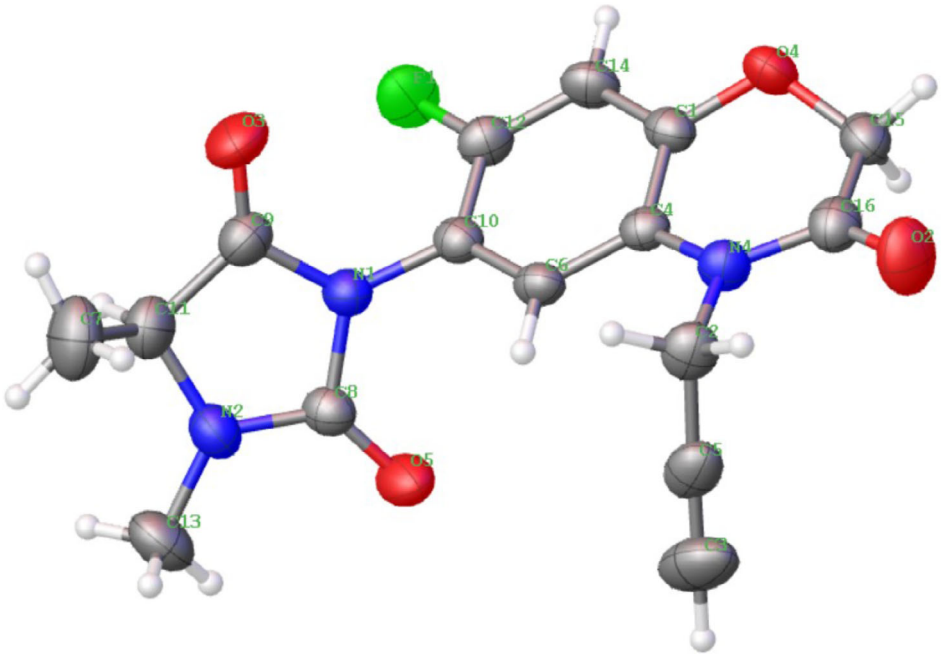

Figure 4. The X-ray crystal structure of compound **A1**.

control, while an emulsion without any inhibitors (composed of DMF and Tween-80) served as the blank control. After a 14-day treatment period, herbicidal activity was assessed through visual evaluation. All experiments were repeated three times. The post-emergence herbicidal activity evaluation data for all tested compounds, including FLU, are shown in Table 1.

2.5 Crop selectivity

To evaluate the crop selectivity of novel benzoxazinone compounds, the compound **A1**, which exhibited the best herbicidal activity, was selected for further crop selectivity test. Six representative crops, including rice, wheat, maize, peanut, cotton, and soybean, were chosen as subjects for the crop selectivity studies. These experimental crops were grown in plastic pots within the greenhouse until they reached the four-leaf stage, at which point they were treated with inhibitor emulsions at dosages ranging from 75 to 150 g ai/ha. The extent of damage was assessed after 21 days. All experiments were conducted in triplicate. The evaluation results are presented in Table 2.

2.6 Molecular docking and binding free energy calculation

According to the reported method,[16,38,39] the crystal structure of *Nt*PPO (PDB ID: 1sez) was downloaded from the PDB database to serve as the receptor for molecular docking studies. Meanwhile, the chemical structures of compounds **A1** and FLU were constructed and optimized. AutoDockTools version 1.5.6 was utilized to prepare the ligands and receptors. AutoDock 4.2 was employed to predict the binding modes between compounds **A1** and FLU and *Nt*PPO. Discovery Studio 2016 was employed to investigate the interactions between the ligand and the key residues of the receptor. PYMOL 1.8.6 was used to display the active site of the inhibitor and to visualize the binding modes from the docking results.

Molecular dynamics (MD) simulations of ligand-protein complexes were carried out using the AMBER 20 software package and the ff19SB force field. The AMBER force fields for the ligands were generated with the Antechamber program, which enables the creation of the AMBER Generalized Force Field (GAFF) for ligands. The ligand-protein systems underwent a gently annealed process from 0 to 300 K in 50 ps, followed by a 50 ps equilibrating calculation at 300 K and 1 atm. Subsequently, each complex was subjected to a 30 ns MD simulation. The last 10 ns of the MD trajectories for each system were used for energy decomposition analysis and binding free energy calculations.

3 RESULTS AND DISCUSSION

3.1 Chemistry

As shown in Fig. 2, intermediates **7a**-**7c** were synthesized following previously reported methods, involving reaction types such as substitution, cyclization, nitration, and reduction of nitro groups.[7] Intermediates **7a**-**7c** and triethylamine were dissolved in 1,4-dioxane, the solution containing intermediates **7a**-**7c** was then slowly added to a solution of triphosgene in 1,4-dioxane at 0–5 °C. After the addition was complete, the mixture was heated to reflux. After a reaction period of approximately 4–6 h, the amino groups were converted to isocyanate groups, yielding intermediates **8a**-**8c**. After the solvent was removed, intermediates **8a**-**8c** were used directly in the subsequent step without purification. Intermediate **8a**-**8c** were dissolved in 1,4-dioxane and reacted with various types of amino acid methyl esters (racemate) at refluxing temperature under basic condition to obtain intermediates **9a**-**9c**. Intermediates **9a**-**9c** were dissolved in a mixed solution of 6 M HCl/CH_3OH (v/v = 1:1) and heated to reflux to obtain the cyclized intermediates **10a**-**10c**.[40] Subsequently, the intermediates **10a**-**10c** were dissolved in DMF and stir with Cs_2CO_3 at 50 °C to finally give the target compounds **A1**-**A15** in good yields.

Simultaneously, the intermediate **7a** (6-amino-7-fluoro-4-(prop-2-yn-1-yl)-2H- benzo[b][1,4]oxazin-3(4H)-one) and 3,4,5,6-tetrahydrophthalic anhydride were dissolved in acetic acid and

Table 1. Chemical structures and post-emergence herbicidal activities of novel benzoxazinone derivatives

Compound	Dosage (g ai/ha)	R^1	R^2	R^3/R^4	Inhibition (%)					
					L.P.	*E.C.*	*D.S.*	*A.R.*	*A.T.*	*M.S.*
10a	150	$CH_2C{\equiv}CH$	CH_3	H	0	0	0	0	0	0
A1	150	$CH_2C{\equiv}CH$	CH_3	CH_3	50	100	100	100	100	100
	75				30	80	70	100	100	90
A2	150	$CH_2C{\equiv}CH$	$CH(CH_3)_2$	CH_3	0	0	0	80	70	70
A3	150	$CH_2C{\equiv}CH$	$CH_2CH(CH_3)_2$	CH_3	0	0	0	50	40	50
A4	150	$CH_2C{\equiv}CH$	$CH_2C_6H_5$	CH_3	0	0	0	0	0	0
A5	150	$CH_2C{\equiv}CH$	CH_3	CH_2CH_3	0	0	0	70	60	50
A6	150	$CH_2C{\equiv}CH$	CH_3	$CH_2CH_2CH_3$	0	0	0	50	50	50
A7	150	$CH_2C{\equiv}CH$	CH_3	$CH_2(CH_2)_2CH_3$	0	0	0	30	30	40
A8	150	$CH_2C{\equiv}CH$	CH_3	$CH_2CH(CH_3)_2$	0	0	0	30	30	30
A9	150	$CH_2C{\equiv}CH$	CH_3	$CH_2CH{=}CH_2$	0	10	10	80	80	60
A10	150	$CH_2C{\equiv}CH$	CH_3	$CH_2CH{=}C(CH_3)_2$	0	10	10	80	70	70
A11	150	$CH_2C{\equiv}CH$	CH_3	$CH_2COOC_2H_5$	0	0	0	10	10	10
A12	150	$CH_2C{\equiv}CH$	CH_3	$CH_2COC_2H_5$	0	0	0	0	0	0
A13	150	$CH_2C{\equiv}CH$	CH_3	$CH_2COC_6H_5$	0	0	0	0	0	0
A14	150	CH_3	CH_3	CH_3	0	0	0	10	10	10
A15	150	$CH_2C_6H_4(4\text{-}OCH_3)$	CH_3	CH_3	0	0	0	10	10	10
B1	150	-	-	CH_2COOH	0	0	0	0	0	0
B2	150	-	-	CH_2COOCH_3	0	20	30	100	80	75
B3	150	-	-	$CH_2COOCH_2CH_3$	0	20	30	100	85	80
B4	150	-	-	CH_2CH_2OH	0	0	10	80	80	60
B5	150	-	-	$CH_2C_6H_5$	40	80	70	100	100	100
FLU	150				90	100	100	100	100	100
	75				70	90	100	100	100	100

Abbreviations: LP, *Lolium perenne*; EC, *Echinochloa crusgalli*; DS, *Digitaria sanguinalis*; AR, *Amaranthus retroflexus*; AT, *Abutilon theophrasti*; MS, Medicago sativa; FLU, Flumioxazin.

Table 2. Post-emergence crop selectivity of compounds **A1** and flumioxazin

Compound	Dosage (g ai/ha)	Crop injury (%)					
		Rice	Wheat	Maize	Peanut	Cotton	Soybean
A1	150	50	60	40	70	100	90
	75	40	30	30	40	90	70
Flumioxazin	150	80	75	70	80	100	100
	75	60	60	50	60	90	85

heated to 80 °C with stirring to prepare FLU. To construct benzoxazinone derivatives containing a 1,2,3-triazoles moiety, copper-catalyzed cyclization reactions were carried out according to reported procedures.[41] FLU and various types of azide compounds were dissolved in 1,4-dioxane, CuI was added as a catalyst, and the mixture was stirred and heated to 80 °C to reaction, yielding the target compounds **B1**-**B5** in excellent yields. The chemical structures of the target compounds were characterized by ^1H, ^{13}C, and ^{19}F NMR spectra, as well HRMS spectra.

3.2 Herbicidal activity and structure–activity relationships (SARs)

The pot-spraying method was utilized to evaluate the post-emergence herbicidal activities of all benzoxazinone derivatives against six representative weeds. The PPO herbicide FLU was selected as the control agent, and the results are shown in Table 1. Initially, we analyzed the SAR of the benzoxazinone compounds based on previous literature and found that replacing the R^1 with a propargyl group may enhance the herbicidal activity.[16] Therefore, the propargyl group was selected as the preferred substituent at the R^1 position. Meanwhile, to construct the hydantoin fragment, various types of racemic amino acid methyl esters were employed in the cyclization reactions and to evaluate the substituent at the R^2 position. Additionally, compounds **A1**-**A4** were synthesized by substituting the NH group on the hydantoin with methyl iodide. We discovered that compound **A1** ($R^2 = CH_3$) exhibited superior herbicidal activity compared to **A2** ($R^2 = CH(CH_3)_2$), **A3** ($R^2 = CH_2CH(CH_3)_2$), and **A4** ($R^2 = CH_2C_6H_5$). Based on these results, we speculate that the introduction of long-chained alkyl groups or bulky aryl substituents at the R^2 position

may significantly reduce the herbicidal activity of the compounds. Subsequently, we investigated the effect of different substituents at the R^3 position on their herbicidal activities. The results indicate that introducing different alkyl groups at the R^3 position (**A5**-**A8**) could decrease the herbicidal activity, which might be influenced by the increasing steric hindrance. For example, the compound **A1** ($R^3 = CH_3$) displayed high efficiency and broad-spectrum herbicidal activity. In contrast, the compounds synthesized by nucleophilic substitution of NH with long-chain haloalkanes (**A5**-**A8**) exhibited limited inhibition effects on the growth of broadleaf weeds and only slight inhibitory effects on gramineous weeds. It is noteworthy that when the R^3 position was substituted with alkenyl groups (**A9**-**A10**), the herbicidal activities were slightly higher than that of compounds **A5**-**A8**, but still exhibited weak herbicidal activity against gramineous weeds. When the R^3 position was occupied by ester or carbonyl substituents (**A11**-**A13**), the herbicidal activity of the synthesized compounds was very weak, only exhibiting slight symptoms in the early stages. To investigate the importance of the methyl group at the R^3 position, we assessed the herbicidal activity of intermediate **10a**. We found intermediate **10a** exhibited almost negligible herbicidal activity against all weeds. Finally, we investigated the impact of R^1 substituents on herbicidal activity using methyl and benzyl groups (**A14**-**A15**), and only slight injury to broadleaf weeds is observed. This finding is consistent with previous reports in the literature. Therefore, we did not explore the diversity of substituents on the NH of benzoxazinone. Finally, through systematic screening of herbicidal activity, we found that compound **A1** exhibited 100% herbicidal activity against *Echinochloa crusgalli*, *Digitaria sanguinalis*, *Amaranthus retroflexus*, *Abutilon theophrasti*, and *Medicago sativa* at a dose of 150 g ai/ha. Furthermore, at a reduced dose of 75 g ai/ha, it still exhibited over 90% herbicidal activity against broadleaf weeds.

Meanwhile, we investigated the herbicidal activity of benzoxazinone derivatives that contain a 1,2,3-triazole fragment. We discovered that different types of branched substituents derived from 1,2,3-triazole exhibited significant influence on herbicidal activity. For example, the compound **B1**, which bears a carboxyl group on the 1,2,3-triazole motif, demonstrated negligible herbicidal activity. This may be attributed to its poor solubility and lipophilicity. The formation of precipitation of **B1** in the emulsion supports our deduction. In contrast, the herbicidal activity is markedly enhanced when ester groups were introduced to the 1,2,3-triazole moiety, especially against broadleaf weeds. For example, compounds **B2** and **B3** exhibit over 75% herbicidal activity against *Amaranthus retroflexus*, *Abutilon theophrasti*, and *Medicago sativa* at a dosage of 150 g ai/ha, while demonstrating weak activity against *Echinochloa crusgalli* and *Digitaria sanguinalis*. Moreover, the introduction of hydroxyethyl group on the branched chain of 1,2,3-triazole (**B4**) also demonstrated moderate to good herbicidal activity against broadleaf weeds. Interestingly, the compound **B5**, synthesized from (azidomethyl)benzene and FLU, demonstrated 100% herbicidal activity against the tested broadleaf weeds at a dosage of 150 g ai/ha and over 70% herbicidal activity against *Echinochloa crusgalli* and *Digitaria sanguinalis*. Unfortunately, it exhibited only 40% herbicidal activity against *Lolium perenne*.

Based on the above analysis, we next systematically studied the effects of the R^2 and R^3 groups on the benzoxazinone derivatives containing a hydantoin fragment (**A1**-**A15**). The results indicated that the methyl substituents at both the R^2 and R^3 positions benefited the herbicidal activity. The herbicidal activities decreased when switching the R^3 group into other substituents: methyl group > unsaturated hydrocarbons > saturated alkanes > ester groups > H. A propargyl group at the R^1 position exhibited better herbicidal effects than the other substituents we tested. For benzoxazinone derivatives containing a 1,2,3-triazole moiety, the branched substituents attached to the 1,2,3-triazole fragment play a vital role in the herbicidal activity of the compounds. Our preliminary analysis indicated that the presence of a benzyl group and an ester group attached to the 1,2,3-triazole moiety enhanced the herbicidal activity of the compounds. However, due to the limited number of novel benzoxazinone derivatives that incorporate 1,2,3-triazole fragments, further investigation is needed to explore and discover new compounds with high herbicidal activity. The SAR analysis of the synthesized novel benzoxazinone derivatives is shown in Fig. 5.

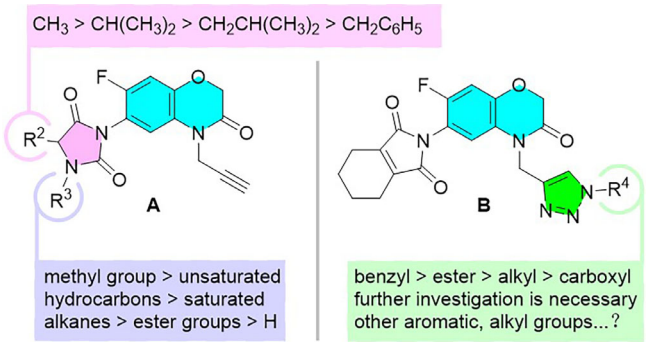

Figure 5. SAR analysis of novel benzoxazinone derivatives as herbicides.

3.3 Crop selectivity

To evaluate the commercializing potential of the current benzoxazinone derivatives, we assessed the post-emergence crop selectivity of the representative compound **A1**. The selectivity evaluation data of compound **A1** and FLU against rice, wheat, corn, peanut, cotton, and soybean at application doses of 75–150 g ai/ha are shown in Table 2. It is noteworthy that all crops treated with compound **A1** and FLU exhibit severe burn symptoms at early stages. However, in the later stages, different crops exhibited varying degrees of recovery. Within the dosage range of 75–150 g ai/ha, compound **A1** exhibited overall greater safety to the tested crops than the control drug of FLU. At a dosage of 150 g ai/ha, there was no significant difference in safety between compound **A1** and FLU for dicotyledonous crops. In contrast, compound **A1** demonstrated obviously superior safety for monocotyledonous crops to FLU. When the application rate is reduced to 75 g ai/ha, the safety of compound **A1** significantly increases in rice, wheat, maize, and peanuts, with a damage rate of only 30% observed in wheat and maize. The results of the herbicidal activity and crop selectivity assessments suggest that compound **A1** possesses great potential for commercialization as a novel PPO-inhibiting herbicide.

3.4 Molecular simulation studies

To gain a deeper understanding of the herbicidal mechanism of the highly active compound **A1**, we selected compounds **A1** and FLU for subsequent molecular simulation studies. As shown in Table 3, the binding free energies of the **A1** – *Nt*PPO and flumioxazin–*Nt*PPO systems were calculated using the MM_PBSA method. The ΔE_{ele} values for the **A1** – *Nt*PPO and flumioxazin –*Nt*PPO systems were −40.15 kcal/mol and −55.81 kcal/mol,

Table 3. Binding energies (kcal/mol) of compound **A1** and flumioxazin with *Nt*PPO

Compound	ΔE_{ele}	ΔE_{vdw}	ΔE_{MM}[a]	ΔE_{sol}	ΔE_{bind}[b]	$-T\Delta S$	ΔG_{bind}[c]
A1	−40.15	−46.06	−86.21	41.75	−44.46	20.13	−24.33
Flumioxazin	−55.81	−26.57	−82.37	37.21	−45.16	10.28	−34.88

[a] $\Delta E_{MM} = \Delta E_{ele} + \Delta E_{vdw}$.
[b] $\Delta E_{bind} = \Delta E_{gas} + \Delta G_{sol}$.
[c] $\Delta G_{bind} = \Delta E_{bind} - T\Delta S$.

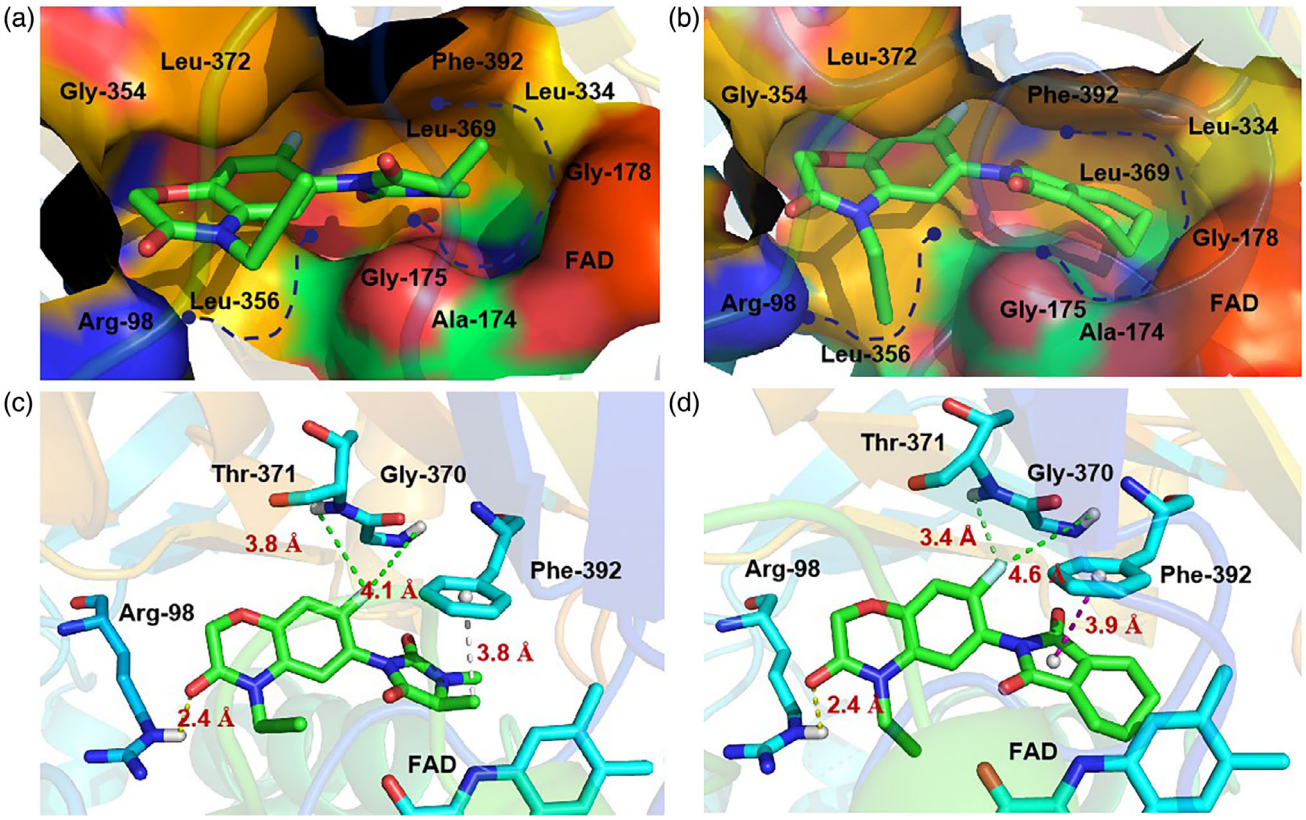

Figure 6. Active cavity and binding modes of compounds **A1** and Flumioxazin with *Nt*PPO. Active cavity and binding modes of compound **A1** with *Nt*PPO (A and C), Active cavity and binding modes of flumioxazin with *Nt*PPO (B and D). The compounds **A1** and flumioxazin are shown as green sticks. The key residues around the active site and FAD are shown in blue sticks.

respectively, which indicated that the electrostatic energy of flumioxazin (including hydrogen bond interactions) with *Nt*PPO is greater than that of compound **A1** with *Nt*PPO. Besides, the ΔE_{vdw} value for compound **A1** (−46.06 kcal/mol) was higher than that of FLU (−26.57 kcal/mol) when interacting with *Nt*PPO. In addition, the binding free energies (ΔG_{bind}) of compound **A1** and FLU with *Nt*PPO were −24.33 kcal/mol and −34.88 kcal/mol, respectively. This indicates that FLU binds more tightly to *Nt*PPO than compound **A1**, which is consistent with the results of the herbicidal activity assays.

To visually illustrate the binding mode of compound **A1** with *Nt*PPO, the molecular docking results of compound **A1** and FLU are presented in Fig. 6. We observed that compound **A1** and FLU bind to *Nt*PPO within the same hydrophobic pocket, surrounded by several hydrophobic residues, including Leu-334, Leu-356, Leu-369, Leu-372, and Phe-392 (Fig. 6(A),(B)). Therefore, they may exhibit similar types of interaction to these amino acid residues (Fig. 6(C),(D)). For example, the carbonyl group of the oxazinone in compound **A1** and FLU engages in a hydrogen bond interaction with Arg-98, with a bond length of 2.4 Å. In addition, the fluorine atom on the benzene ring of compound **A1** forms hydrogen bonds with Gly-370 and Thr-371, exhibiting bond lengths of 4.1 Å (F···Gly-370) and 3.8 Å (F···Thr-371). Meanwhile, in FLU, the fluorine atom also establishes hydrogen bonds with Gly-370 and Thr-371, with bond lengths of 4.6 and 3.4 Å, respectively. Besides, the difference is that the five-membered ring of the cyclic imide moiety in the structure of FLU possesses aromaticity, which enables it to form a π-π stacking interaction with Phe-392, characterized by a bond length of 3.9 Å. However, one of the methyl groups on the hydantoin fragment of compound **A1** forms a π-alkyl interaction with Phe-392, with a distance of 3.8 Å. To gain a more detailed insight into the contribution of each residue in *Nt*PPO to the binding free energy, we decomposed the binding free energy of the **A1**-*Nt*PPO and flumioxazin-*Nt*PPO

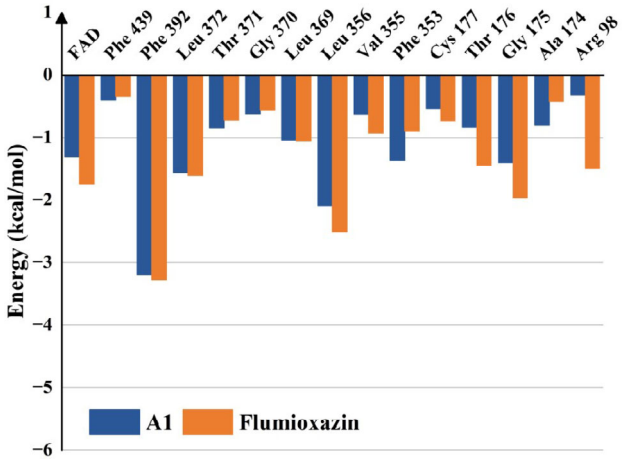

Figure 7. Decomposition of the binding free energy (kcal/mol) between compounds **A1** and flumioxazin with *Nt*PPO.

systems. As shown in Fig. 7, the contributions to the binding free energy primarily originated from the residues Arg-98, Gly-175, Thr-176, Phe-353, Leu-356, Leu-369, Leu-372, and Phe-392. Among these residues, Phe-392 serves as the most significant contributing residue, exhibiting binding energies of −3.20 kcal/mol and −3.28 kcal/mol for the **A1**-*Nt*PPO and flumioxazin-*Nt*PPO complexes, respectively. These results highlight the importance of the van der Waals interactions between Phe-392 and the hydantoin moiety in compound **A1**, as well as the five-membered ring in FLU. Meanwhile, the high PPO inhibition rate of compound **A4** may also be enhanced by a stronger van der Waals interaction between the phenyl group on the hydantoin moiety and Phe-392. Furthermore, the binding energies for the residue Leu-356 in the **A1**-NtPPO and flumioxazin-*Nt*PPO systems are −2.09 kcal/mol and −2.51 kcal/mol, suggesting that the propargyl also contributes significantly to the van der Waals interactions. The multiple computational analyses of the binding modes of novel benzoxazinone derivatives within the active pocket of *Nt*PPO have provided in-depth insights and theoretical guidance for the rational design of novel PPO inhibitors.

In summary, we designed and synthesized a series of structurally novel benzoxazinone derivatives as novel PPO inhibitors by incorporating hydantoin or 1,2,3-triazole fragments into the benzoxazinone scaffold. Through systematic screening of the herbicidal activity of all synthesized target compounds, we found that compound **A1** exhibited 100% herbicidal activity against *Echinochloa crusgalli*, *Digitaria sanguinalis*, *Amaranthus retroflexus*, *Abutilon theophrasti*, and *Medicago sativa* at a dose of 150 g ai/ha. Furthermore, at a reduced dose of 75 g ai/ha, it still demonstrated over 90% herbicidal activity against broadleaf weeds. Additionally, crop selectivity experiments indicated that compound **A1** has the potential for application in wheat and corn fields. Molecular docking results indicated that compound **A1** and FLU occupy the same active site of the *Nt*PPO enzyme and exhibit similar interactions with the same residues. Overall, this valuable finding provides new insights for the future development of novel benzoxazinone derivatives as PPO inhibitors.

FUNDING INFORMATION

We acknowledge financial support from the National Natural Science Foundation of China (22371058, 22371057, 32172459, 22071036). National Natural Science Fund for Excellent Young Scientists Fund Program (Overseas), the starting grant of Guizhou University [(2023)29)]. Science and Technology Department of Guizhou Province (Qiankehejichu-ZK [2021]Key033). The Central Government Guides Local Science and Technology Development Fund Projects [Qiankehezhongyindi (2024)007, (2023)001]. The Program of Major Scientific and Technological, Guizou Province [Qiankehechengguo(2024)zhongda007]. The 10 Talent Plan (Shicengci) of Guizhou Province ([2016]5649). The Program of Introducing Talents of Discipline to Universities of China (111 Program, D20023) at Guizhou University. Yongjiang Plan for Innovation and Entrepreneurship Leading Talent Project in the City of Nanning (2021005).

DATA AVAILABILITY STATEMENT

The data that supports the findings of this study are available in the supplementary material of this article.

CONFLICTS OF INTEREST

The authors declare no competing financial interest.

SUPPORTING INFORMATION

Supporting information may be found in the online version of this article.

REFERENCES

1 Zhang F, Tang W, Hedtke B, Zhong L, Liu L, Peng L *et al.*, Tetrapyrrole biosynthetic enzyme protoporphyrinogen IX oxidase 1 is required for plastid RNA editing. *Proc Natl Acad Sci USA* **111**:2023–2028 (2014).
2 Brzezowski P, Ksas B, Havaux M, Grimm B, Chazaux M, Peltier G *et al.*, The function of protoporphyrinogen IX oxidase in chlorophyll biosynthesis requires oxidised plastoquinone in Chlamydomonas reinhardtii. *Commun Biol* **2**:159–168 (2019).
3 Ambrosini V, Issawi M, Leroy-Lhez S and Riou C, How protoporphyrinogen IX oxidase inhibitors and transgenesis contribute to elucidate plant tetrapyrrole pathway. *J Porphyrins Phthalocyanines* **23**:419–426 (2019).
4 Yih RY and Swithenbank C, New potent diphenyl ether herbicides. *J Agric Food Chem* **23**:592–593 (1975).
5 Giacomini DA, Umphres AM, Nie H, Mueller TC, Steckel LE, Young BG *et al.*, Two new PPX2 mutations associated with resistance to PPO-inhibiting herbicides in Amaranthus palmeri. *Pest Manag Sci* **73**:1559–1563 (2017).
6 Rangani G, Salas-Perez RA, Aponte RA, Knapp M, Craig IR, Mietzner T *et al.*, Novel single-site mutation in the catalytic domain of Protoporphyrinogen oxidase IX (PPO) confers resistance to PPO-inhibiting herbicides. *Front Plant Sci* **10**:568–580 (2019).
7 Wang DW, Li Q, Wen K, Ismail I, Liu DD, Niu CW *et al.*, Synthesis and herbicidal activity of pyrido[2,3-d]pyrimidine-2,4-dione–benzoxazinone hybrids as protoporphyrinogen oxidase inhibitors. *J Agric Food Chem* **65**:5278–5286 (2017).
8 Zhao LX, Chen KY, He XL, Zou YL, Gao S, Fu Y *et al.*, Design, synthesis, and biological activity determination of novel phenylpyrazole protoporphyrinogen oxidase inhibitor herbicides containing five-membered heterocycles. *J Agric Food Chem* **71**:14164–14178 (2023).
9 Dayan FE, Barker A and Tranel PJ, Origins and structure of chloroplastic and mitochondrial plant protoporphyrinogen oxidases: implications for the evolution of herbicide resistance. *Pest Manag Sci* **74**:2226–2234 (2018).
10 Zuo Y, Wu Q, Su SW, Niu CW, Xi Z and Yang GF, Synthesis, herbicidal activity, and QSAR of novel N-Benzothiazolyl-pyrimidine-2,4-diones as protoporphyrinogen oxidase inhibitors. *J Agric Food Chem* **64**:552–562 (2016).
11 Hao GF, Zuo Y, Yang SG, Chen Q, Zhang Y, Yin CY *et al.*, Computational discovery of potent and bioselective protoporphyrinogen IX oxidase

inhibitor via fragment deconstruction analysis. *J Agric Food Chem* **65**: 5581–5588 (2017).
12 Jiang LL, Tan Y, Zhu XL, Wang ZF, Zuo Y, Chen Q *et al*., Design, synthesis, and 3D-QSAR analysis of novel 1,3,4-oxadiazol-2(3H)-ones as protoporphyrinogen oxidase inhibitors. *J Agric Food Chem* **58**: 2643–2651 (2010).
13 Zheng BF, Wang ZZ, Dong J, Ma JY, Zuo Y, Wu QY *et al*., Discovery of a Subnanomolar inhibitor of Protoporphyrinogen IX oxidase via fragment-based virtual screening. *J Agric Food Chem* **71**:8746–8756 (2023).
14 Zhang H, Liu K, Liu R, Li Q, Li Y, Wang Q *et al*., Design, synthesis and herbicidal activities of Tetrahydroisoindoline-1,3-dione derivatives containing Alkoxycarbonyl substituted 2-Benzoxazolinone. *Chin J Chem* **33**:749–755 (2015).
15 Zheng BF, Zuo Y, Yang WY, Liu H, Wu QY and Yang GF, Design, synthesis, and biological evaluation of Pyridazinone-containing derivatives As novel Protoporphyrinogen IX oxidase inhibitor. *J Agric Food Chem* **72**:10772–10780 (2024).
16 Wang DW, Zhang H, Yu SY, Zhang RB, Liang L, Wang X *et al*., Discovery of a potent thieno[2,3-d]pyrimidine-2,4-dione-based protoporphyrinogen IX oxidase inhibitor through an in silico structure-guided optimization approach. *J Agric Food Chem* **69**:14115–14125 (2021).
17 Konnert L, Lamaty F, Martinez J and Colacino E, Recent advances in the synthesis of Hydantoins: the state of the art of a valuable scaffold. *Chem Rev* **117**:13757–13809 (2017).
18 Cho S, Kim SH and Shin D, Recent applications of hydantoin and thiohydantoin in medicinal chemistry. *Eur J Med Chem* **164**:517–545 (2019).
19 Aryal S, Hone CA, Polson MIJ and Foley DJ, Enantioselective synthesis of hydantoins by chiral acid-catalysed condensation of glyoxals and ureas. *Chem Sci* **14**:7905–7912 (2023).
20 Barve IJ, Dalvi PB, Thikekar TU, Chanda K, Liu YL, Fang CP *et al*., Design, synthesis and diversification of natural product-inspired hydantoin-fused tetrahydroazepino indoles. *RSC Adv* **5**:73169–73179 (2015).
21 Lalezari I, One-step synthesis of 3-amino-2,4-imidazolinediones (3-aminohydantoins) from α-amino acids. *J Heterocyclic Chem* **22**:741–743 (1985).
22 Williamson KS, Michaelis DJ and Yoon TP, Advances in the chemistry of Oxaziridines. *Chem Rev* **114**:8016–8036 (2014).
23 Wang Y, Luo X, Chen Y, Peng J, Yi C and Chen J, Recent research progress of heterocyclic nematicidal active compounds. *J Heterocyclic Chem* **60**:1287–1300 (2023). https://doi.org/10.1002/jhet.4616.
24 Kerru N, Gummidi L, Maddila S, Gangu KK and Jonnalagadda SB, A review on recent advances in nitrogen-containing molecules and their biological applications. *Molecules* **25**:1909–1950 (2020).
25 Yang TL, Dong J, Wang XL, Dong J and Lin HY, Discovery of 4-Hydroxyphenylpyruvate dioxygenase inhibitors with novel pharmacophores. *Adv Agrochem* **3**:344–350 (2024).
26 Peng L, Chen J, Chen Y, Lu H, Okuda Y, Tang Z *et al*., Sulfur-containing 1,2,3-Triazoles: synthesis and properties. *Eur J Org Chem* **27**: e202301146 (2024). https://doi.org/10.1002/ejoc.202301146.
27 Zhou CH and Wang Y, Recent researches in Triazole compounds as medicinal drugs. *Curr Med Chem* **19**:239–280 (2012). https://doi.org/10.2174/092986712803414213.
28 Jiang Y, Zhu CH, Xia ZH and Zhao HQ, Novel quinoxalinone-1,-2,3-triazole derivatives as potential antifungal agents for plant anthrax disease: design, synthesis, antifungal activity and SAR study. *Adv Agrochem* **3**:222–228 (2024).
29 Xu Z, Zhao SJ and Liu Y, 1,2,3-Triazole-containing hybrids as potential anticancer agents: current developments, action mechanisms and structure-activity relationships. *Eur J Med Chem* **183**:11700–11736 (2019). https://doi.org/10.1016/j.ejmech.2019.111700.
30 Dheer D, Singh V and Shankar R, Medicinal attributes of 1,2,3-triazoles: current developments. *Bioorg Chem* **71**:30–54 (2017).
31 Singh MS, Chowdhury S and Koley S, Advances of azide-alkyne cycloaddition-click chemistry over the recent decade. *Tetrahedron* **72**:5257–5283 (2016).
32 Wang C, Yang J and Lu Y, Click chemistry as a connection tool: grand opportunities and challenges. *Chin J Catal* **49**:8–15 (2023).
33 Jin J, Mou C, Zou J, Xie X, Wang C, Shen T *et al*., Development of axially chiral urazole scaffolds for antiplant virus applications against potato virus Y. *Pest Manag Sci* **79**:2527–2538 (2023). https://doi.org/10.1002/ps.7428.
34 Lv Y, Luo G, Liu Q, Jin Z, Zhang X and Chi YR, Catalytic atroposelective synthesis of axially chiral benzonitriles via chirality control during bond dissociation and CN group formation. *Nat Commun* **13**:36–45 (2022). https://doi.org/10.1038/s41467-021-27813-4.
35 Tang C, Cai H, Song C, Wang X, Jin Z and Li T, N-heterocyclic Carbene-catalyzed Regio- and enantioselective C7-alkylation of 4-Aminoindoles with α-Bromoenals. *Org Lett* **26**:1787–1791 (2024).
36 Zhao LX, Wang ZX, Zou YL, Gao S, Fu Y and Ye F, Phenoxypyridine derivatives containing natural product coumarins with allelopathy as novel and promising protoporphyrin IX oxidase-inhibiting herbicides: design, synthesis and biological activity study. *Pestic Biochem Physiol* **177**:104897–104907 (2021). https://doi.org/10.1016/j.pestbp.2021.104897.
37 Cai H, Zhang X, Ling D, Zhang M, Pang C, Chen Z *et al*., Discovery of Pyridyl-Benzothiazol hybrids as novel Protoporphyrinogen oxidase inhibitors via scaffold hopping. *J Agric Food Chem* **72**:8963–8972 (2024).
38 Zhao LX, Peng JF, Liu FY, Zou YL, Gao S, Fu Y *et al*., Design, synthesis, and herbicidal activity of diphenyl ether derivatives containing a five-membered heterocycle. *J Agric Food Chem* **70**:1003–1018 (2022).
39 Zheng BF, Zuo Y, Huang GY, Wang ZZ, Ma JY, Wu QY *et al*., Synthesis and biological activity evaluation of benzoxazinone-pyrimidinedione hybrids as potent protoporphyrinogen IX oxidase inhibitor. *J Agric Food Chem* **71**:14221–14231 (2022).
40 Liang T, Hou X, Zhou Y, Yang X and Fang H, Design, synthesis, and biological evaluation of 2,4-Imidazolinedione derivatives as HDAC6 isoform-selective inhibitors. *ACS Med Chem Lett* **10**:1122–1127 (2019).
41 Su CL, Tseng CL, Ramesh C, Liu HS, Huang CY, F Y *et al*., Using gene expression database to uncover biology functions of 1,4-disubstituted 1,2,3-triazole analogues synthesized via a copper (I)-catalyzed reaction. *Eur J Med Chem* **132**:90–107 (2017). https://doi.org/10.1016/j.ejmech.2017.03.034.